Front. Chem. China 2010, 5(2): 178–183
DOI 10.1007/s11458-010-0114-8

RESEARCH ARTICLE

A novel intramolecular charge transfer fluorescent chemosensor highly selective for Cu^{2+} in neutral aqueous solutions

Qingxian LIAO[1,2], Aifang LI[1], Zhao LI[1], Yibin RUAN[1] and Yunbao JIANG (✉)[1]

A selective and sensitive intramolecular charge transfer (ICT) fluorescent chemosensor was designed for Cu^{2+} in neutral aqueous solutions of pH 7.0. The design of this totally water-soluble fluorescent chemosensor was based on the binding motif of Cu^{2+} to aminoacid, which is coupled to an ICT fluorophore bearing a 1,3,4-thiodiazole moiety in the electron acceptor. The formation of a 1:1 complex of Cu^{2+} to 2 was suggested to lead to fluorescence quenching. The quenching obeyed Stern-Volmer theory in neutral aqueous solution of pH 7.0 for Cu^{2+} over 5.0×10^{-7} to 3.0×10^{-5} mol·L^{-1}, with a quenching constant of 1.8×10^5 L·mol^{-1} and a detection limit of 2.0×10^{-7} mol·L^{-1}. The binding of Cu^{2+} to 2 can be fully reversed by addition of chelator EDTA, affording a reversible sensing performance.

Keywords fluorescent chemosensor, Cu^{2+}, fluorescence quenching, intramolecular charge transfer, 1, 3, 4-thiodiazole

1 Introduction

Copper is one of the essential trace elements for human health, playing a vital role in human metabolism process [1]. Facile determination of copper under physiologic conditions is therefore highly demanded. There are many chromogenic and fluorometric approaches reported for the determination of copper [2]. Most of them operated in aqueous solutions containing organic cosolvents [3–26]. To extend the applications to environmental and biologic systems, chemosensors are expected to exhibit high selectivity and sensitivity in aqueous solutions at neutral pH with no organic cosolvents [27–41]. In recent years, we have seen several such Cu^{2+} chemosensors by using polymeric microspheres, quantum dots, and nanomaterials instead of convenient small organic compounds [27–30]. The reported fluorescent organic chemosensors for Cu^{2+} under physiologic conditions are mostly based on peptidyl structures [31–35] or following hydrolysis reactions [36]. The latter can be traced back to the first example of so-called chemodosimeter for Cu^{2+} released by Czarnik et al. that underwent a hydrolysis reaction in the presence of Cu^{2+} [4]. These chemodosimeters provided good Cu^{2+} selectivity, whereas required a reaction-duration. As the chemical reaction is involved, the fluorescent signaling in many cases is irreversible. Small-molecule chemosensors that operate under physiologic conditions remain rare [37–41]. For real-time monitoring of Cu^{2+}, a selective yet reversible small-molecule based fluorescent chemosensor would be preferred.

The design of chelating ligands for selective complexation of metal ions has developed very well due to the exciting developments of supramolecular chemistry. It is known that α-amino acid is a good chelating ligand for Cu^{2+}, we therefore designed an intramolecular charge transfer (ICT) fluorescent chemosensor (**2** in Scheme 1) bearing an aminodiacetate moiety. The latter is linked to the electron acceptor of the ICT fluorophore [42] by a 1,3,4-thiodiazole in which S atom was expected to participate in coordination with Cu^{2+}, considering the thiophilic character of Cu^{2+}. Previously we have reported that **1** (Scheme 1), the precursor of **2**, showed a highly selective response in its emission toward Hg^{2+} [42]. By introducing two acetate terminals into **1**, **2** is totally soluble in water and shows a highly sensitive and selective response toward Cu^{2+} in neutral buffered media in a fluorescence quenching mode. The binding of Cu^{2+} to **2** and the accompanied fluorescence signaling are fast. These processes can be fully reversed by using chelator EDTA, implying a similar binding motif of **2** to that of EDTA toward Cu^{2+}.

2 Experimental

2.1 Apparatus

All fluorescence measurements were carried out on a Hitachi F-4500 spectrofluorometer with excitation and emission slits set at 5.0 nm. Fluorescence quantum yield was measured using quinine sulfate as a standard (Φ_f = 0.546 in 0.5 N H_2SO_4) [43]. Absorption spectra were taken on a Varian CARY-300 UV-Vis spectrophotometer. IR spectra were

Received February 25, 2010; accepted March 15, 2010
1. Department of Chemistry, College of Chemistry and Chemical Engineering, and Key Laboratory of Analytical Sciences, Xiamen University, Xiamen 361005, China
2. Xiamen Water Group Co. Ltd., Xiamen 361008, China
E-mail: ybjiang@xmu.edu.cn

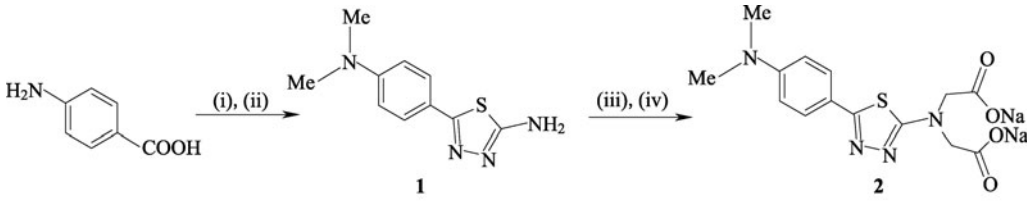

Scheme 1 Synthetic procedures for **2**.

obtained using an Nicolet AVATAR FT-IR360 spectrophotometer (KBr disks). ^{1}H NMR and ^{13}C NMR spectra in D_2O were recorded on a Varian Unity 400 MHz NMR spectrometer. Mass spectra were obtained from a Bruker Micromass-LCT spectrometer. Solution pH was monitored by a Mettler Toledo 320 pH meter calibrated by standard solutions. All of the experiments were carried out at room temperature (25°C).

2.2 Reagents

Solvents and reagents used for the synthesis of the chemosensor were commercially available at AR (analytical reagent) grade. Deionized water was used throughout the experiment. Inorganic nitrate salts were of the highest available purity and were used for preparing their aqueous solutions.

2.3 Synthesis

Chemosensor **2** was synthesized according to Scheme 1 [42,44].

Sodium 2,2′-5-(4-(dimethylamino)phenyl)-1,3,4-thiodiazol-2-ylazanediyl)diacetate (**2**). KI (0.67 g, 4 mmol) and K_2CO_3 (0.71 g, 4 mmol) were added into **1** (0.22 g, 2 mmol) [42] in acetonitrile (CH_3CN, 15 mL) . The resulting mixture was stirred at room temperature while 2 equivalents of ethyl bromoacetate (0.67 g, 4 mmol) were slowly added into the mixture. Refluxing at 70°C was allowed for 4 h. After thin layer chromatography (TLC) indication of the completion of reaction, the mixture was filtered and solvent was evaporated under reduced pressure. Into the residue dissolved in 50 mL ethanol, NaOH (0.3 g, 7.5 mmol) in 2 mL water was added. The resulting solution was refluxed for 3 h. Upon cooling, pale yellow solid was precipitated and was washed, affording **2** (0.3 g) in 80% yield. ^{1}H NMR (D_2O, 400 MHz), δ (ppm): 2.87 (s, 6H), 3.77 (s, 2H), 4.48 (s, 2H), 6.85 (d, J = 8.8 Hz, 2H), 7.50 (d, J = 8.8 Hz, 2H). ^{13}C NMR (D_2O), δ (ppm): 40.0,51.0, 59.6, 113.3, 118.5, 127.2, 148.4, 152.5, 162.4, 175.2, 178.0. HRMS(ESI): calcd for [$C_{14}H_{17}N_4O_4S^+$] *m/z* 337.0971, found (M + H^+, H_2O) 337.0976.

2.4 Absorption and fluorescence measurements

Absorption and fluorescence titrations were performed by adding aliquot Cu^{2+} to a 2 mL solution containing 10 μmol·L^{-1} **2** and 10 mmol·L^{-1} Tris-HCl buffer of pH 7.0. Absorption and fluorescence spectra were recorded after well mixed. Fluorescence intensity was measured at λ_{ex} / λ_{em} = 355 nm / 428 nm.

3 Results and discussion

3.1 Absorption spectra

The absorption spectra of **2** in the presence of various concentration of Cu^{2+} are shown in Figure 1. It was found that the major absorption peak of **2** was blue-shifted from 350 to 339 nm upon the addition of Cu^{2+}, while a tail extending beyond 400 nm was developed. In the titration traces, two clear isosbestic points were observed at 355 and 396 nm,

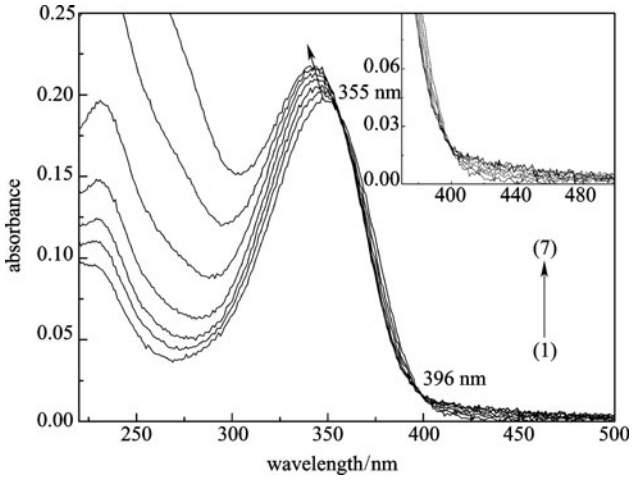

Figure 1 UV-Vis absorption spectra of **2** upon the addition of increasing concentration of Cu^{2+} in 10 mmol·L^{-1} Tris-HCl buffer (pH 7.0). [**2**] = 1.0×10^{-5} mol·L^{-1}. Cu^{2+} ion concentrations were (1) 0 (2) 5.0×10^{-6} mol·L^{-1}, (3) 1.0×10^{-5} mol·L^{-1}, (4) 2.0×10^{-5} mol·L^{-1}, (5) 4.0×10^{-5} mol·L^{-1}, (6) 7.5×10^{-5} mol·L^{-1}, and (7) 1.0×10^{-4} mol·L^{-1}, respectively.

respectively. This is an indication of the formation of well-defined complex between Cu^{2+} and **2**. On the basis of the structure of **2**, the appearance of red-shifted absorption is indicative of an increase in the electron accepting ability of the electron acceptor. It is understandable as Cu^{2+} would bind at its aminodiacetate moiety among others and would agree with the observed red-shift in the absorption spectrum of **1** in the presence of Hg^{2+} [42].

3.2 Fluorescence properties

Fluorescence of **2** was investigated at a physiologic pH 7.0 in Tris-HCl buffer. In the absence of Cu^{2+}, the fluorescence quantum yield of **2** was determined to be 0.0572, which is lower than that of **1** [42], suggesting the occurrence of ICT in **2** in aqueous solution. The ICT character of the emissive state of **2** was confirmed by a solvatochromism measurement. Figure 2 shows that the fluorescence spectrum of **2** continuously shifts to the red in CH_3CN-water binary mixture when water content is increased, being 408 nm in CH_3CN and 428 nm in Tris-HCl buffer solution. In the presence of Cu^{2+}, fluorescence of **2** in Tris-HCl buffer (pH 7.0) was found quenched (Figure 3). No band shift was observed, which means that the formation of a nonfluorescent complex of **2** with Cu^{2+} is responsible for the quenching.

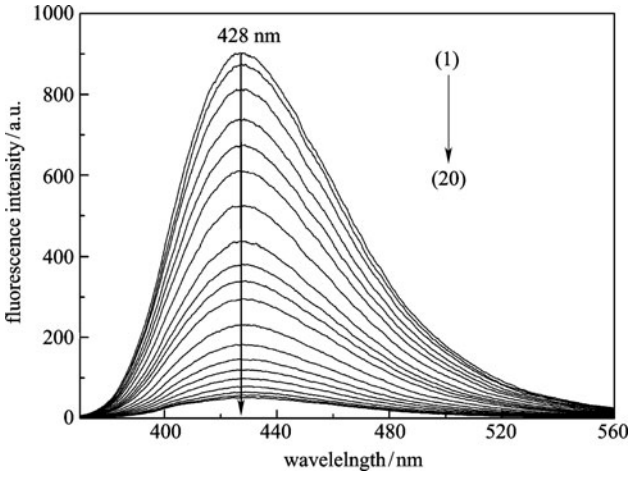

Figure 3 Fluorescence spectra of **2** in the presence of Cu^{2+} in 10 mmol·L^{-1} pH 7.0 Tris-HCl buffer. Cu^{2+} ion concentrations were (1) 0, (2) 5.0×10^{-7} mol·L^{-1}, (3) 1.0×10^{-6} mol·L^{-1}, (4) 2.0×10^{-6} mol·L^{-1}, (5) 3.0×10^{-6} mol·L^{-1}, (6) 4.0×10^{-6} mol·L^{-1}, (7) 6.0×10^{-6} mol·L^{-1}, (8) 7.0×10^{-6} mol·L^{-1}, (9) 8.0×10^{-6} mol·L^{-1}, (10) 1.0×10^{-5} mol·L^{-1}, (11) 1.2×10^{-5} mol·L^{-1}, (12) 1.5×10^{-5} mol·L^{-1}, (13) 2.0×10^{-5} mol·L^{-1}, (14) 3.0×10^{-5} mol·L^{-1}, (15) 5.0×10^{-5} mol·L^{-1}, (16) 1.0×10^{-4} mol·L^{-1}, (17) 1.25×10^{-4} mol·L^{-1}, (18) 1.5×10^{-4} mol·L^{-1}, (19) 2.0×10^{-4} mol·L^{-1}, and (20) 2.5×10^{-4} mol·L^{-1}, respectively. [**2**] = 1.0×10^{-5} mol·L^{-1}. Excitation was chosen at an isosbestic wavelength of 355 nm.

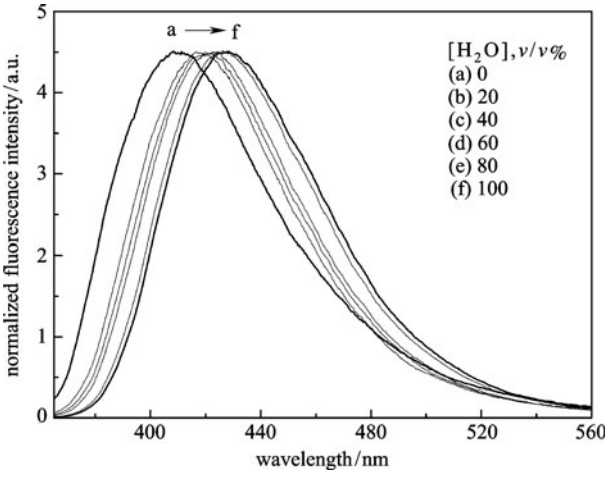

Figure 2 Normalized fluorescence spectra of **2** in CH_3CN and Tris-HCl buffer binary mixture.

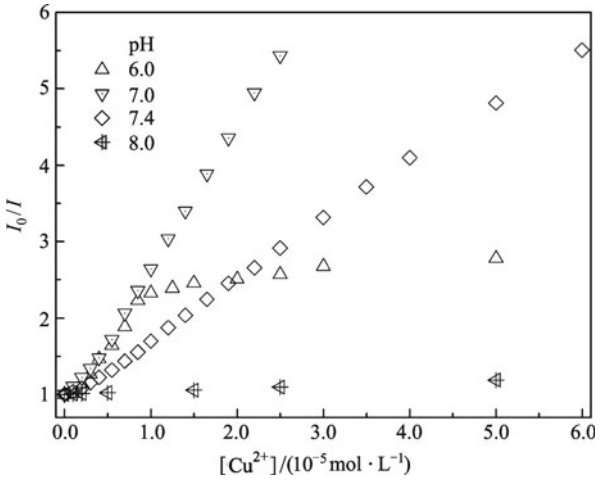

Figure 4 Plots of I_0/I of **2** versus Cu^{2+} concentration in aqueous solution of varied pH. I_0 and I are fluorescence intensities of **2** in the absence and presence of Cu^{2+}, respectively.

3.3 Linear range and selectivity

In order to optimize experimental conditions, several possible factors affecting the measurement of Cu^{2+} were examined in terms of chemosensor concentration, buffer solution pH, and reaction time. Experiments showed that the extent of quenching was highest at pH 7.0 (Figure 4). Tested buffer systems such as HEPES, Tris-HCl, and phosphates all produced optimal results at pH 7.0. Tris-HCl buffer of pH 7.0 was therefore employed. The interaction of **2** with Cu^{2+} was found instant and the fluorescence intensity remained strictly unaltered within 1 h. The concentration of **2** was varied to achieve a credible and wide dynamic range in which Stern-Volmer quenching can be observed. It can found that **2** at 1.0×10^{-5} mol·L^{-1} was the optimal choice. Fluorescence response

of **2** toward Cu^{2+} in terms of quenching factor was found linear to Cu^{2+} concentration ranging from 5.0×10^{-7} to 3.0×10^{-5} mol·L^{-1} ($I_0/I = 0.85 + 1.81 \times 10^5 \times [Cu^{2+}]$, $R = 0.9989$, Figure 3). The detection limit of the chemosensor is defined by the concentration of Cu^{2+} giving a signal equal to the sum of blank signal and three standard deviation of the blank [45,46]. It was 2.0×10^{-7} mol·L^{-1}. The tested foreign metal cations (except Ni^{2+}) showed practically no interference (Figure 5). This observation suggests that **2** is a highly sensitive and selective fluorescent chemosensor for Cu^{2+} in neutral buffered solutions.

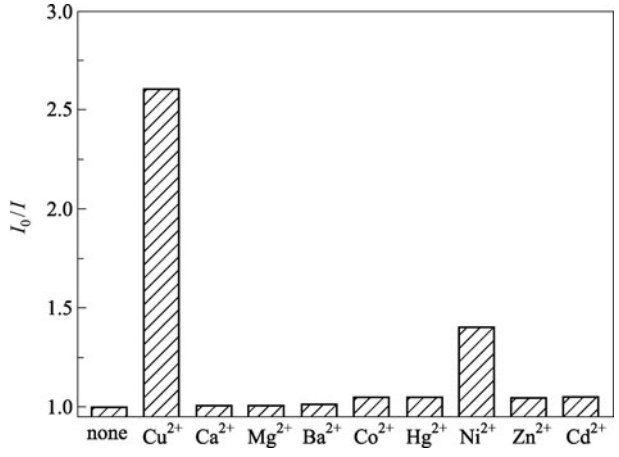

Figure 5 Quenching factor I_0/I of **2** of individual metal ion in pH 7.0 Tris-HCl buffer solution. Cu^{2+} (1.0×10^{-5} mol·L^{-1}), Ca^{2+}, Mg^{2+}, Ba^{2+} (4.0×10^{-4} mol·L^{-1}), Co^{2+}, Hg^{2+}, Zn^{2+} (2.0×10^{-5} mol·L^{-1}), Cd^{2+} (5.0×10^{-5} mol·L^{-1}), Ni^{2+} (1.0×10^{-5} mol·L^{-1}). I and I_0 are fluorescence intensities of **2** in the presence and absence of metal ion, respectively. [**2**] = 1.0×10^{-5} mol·L^{-1}.

3.4 Quenching mechanisms

The observation of isosbestic points in the absorption titration traces suggested the formation of a well-defined complex between **2** and Cu^{2+}, which we confirmed from the Job plot to be of 1:1 stoichiometry (Figure 6). To achieve this 1:1 binding stoichiometry, carbonyl O and amino N of **2** are the most possible binding sites for Cu^{2+}. Actually, IR measurements showed that the carbonyl stretching band shifted from 1608 cm^{-1} in **2** to 1598 cm^{-1} in **2** + Cu^{2+}, which was in agreement with the expected coordination of aminodiacetate moiety with Cu^{2+} [37,38,41]. With **1**, it was suggested that both the 2-amino N atom and the S atom were involved in its coordination with Hg^{2+} [42]. Considering a similar thiophilic character of Cu^{2+} to Hg^{2+}, S atom in **2** was assumed to be coordinating with Cu^{2+}. This would strengthen the electron acceptor of **2** upon the Cu^{2+} binding, the red-shifted absorption tail might be the result of this enhancement. As a consequence, quenching of the fluorescence of **2** would be expected due to a substantially enhanced ICT in the **2**-Cu^{2+} complex, as observed experimentally (Figure 3). Since Cu^{2+} is a heavy transition metal cation, quenching of the fluorescence of **2** by Cu^{2+} can also be due to a heavy atom effect. Although this seems to be less likely in current case as the other heavier Hg^{2+} does not quench the fluorescence of **2** under the same conditions (Figure 5), at this stage we are unable to completely rule out this possibility for Cu^{2+}. It was interesting to note that the binding of Cu^{2+} to **2** and the resulting fluorescence quenching can be fully reversed by adding EDTA (Figure 7). Again this is indicative of the formation of a nonfluorescent complex of **2**-Cu^{2+}, which is responsible for the fluorescence quenching and a similar binding motif of **2** to EDTA toward Cu^{2+}. This reversibility also renders the sensing system reversible. It is significant to

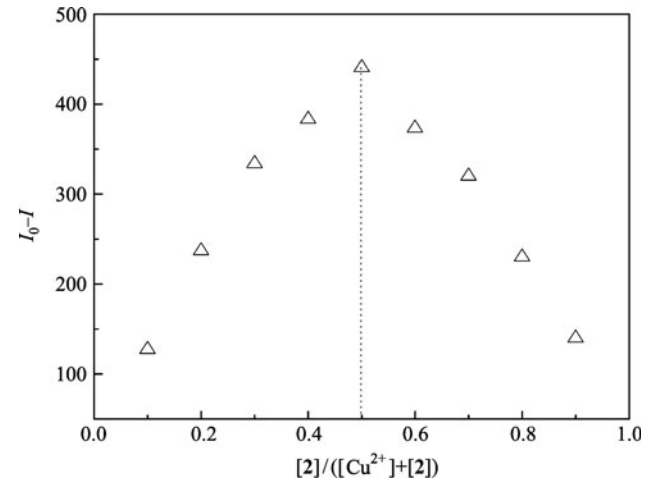

Figure 6 The Job plot for Cu^{2+} binding to **2** in Tris-HCl buffer (pH 7.0). Total concentration of **2** and Cu^{2+} was 2.0×10^{-5} mol·L^{-1}.

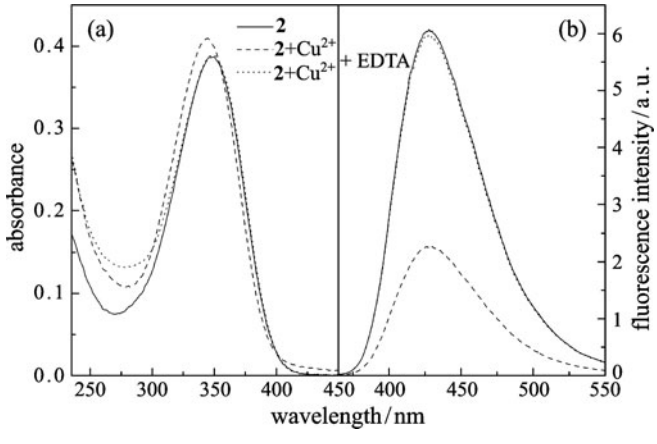

Figure 7 (a) Absorption and (b) fluorescence spectra of **2** in the absence and presence of Cu^{2+} and Cu^{2+} plus EDTA.

point out that by slight modification of the structure of **1** into **2**, we successfully tune the response selectivity from Hg^{2+} to Cu^{2+}. As there are both N and S coordination centers in the 1,3,4-thiodiazole electron acceptor in the structural framework of **1** and **2**, diverse structural motifs can be created to act as fluorescent chemosensors for given metal cations. This shall be the subject of continuing effort.

4 Conclusions

Although many fluorescent chemosensors for Cu^{2+} can be found in literature, those fully soluble in water and operative in neutral aqueous solutions, yet highly sensitive and selective, remain rare. We reported here a highly selective and sensitive ICT fluorescent chemosensor **2** for Cu^{2+} in neutral aqueous solutions. This sensor molecule consisted of an ICT fluorophore and an aminodiacetate binding site that is coupled to the electron acceptor of the ICT fluorophore via a 1,3,4-thiodiazole group, thereby being fully soluble in water. The 2-NH_2 and 1,3,4-thiodiazole moieties provide a nice combination for sophisticated choice of structural modifications in order to achieve a chemosensor selective for a given metal cation. Our results showed that a slight modification of **1** into **2** switched the response selectivity from Hg^{2+} to Cu^{2+}. Highly sensitive dependence of the ICT fluorescence on the electron acceptor/donor ability [47] assures a high sensitivity for sensing when the binding site is incorporated into either the acceptor or the donor. Since other entries of structural modifications are immediately available, the importance of the current versatile structural framework for potential extensions in further designation of sophisticated fluorescent chemosensors of practical significance could be expected.

Acknowledgements We thank the support of the National Natural Science Foundation of China (Grant No. 20835005).

Yunbao JIANG studied chemistry in Xiamen University and received his Ph.D. degree there in 1990 under the supervision of late Prof. Guo-Zhen Chen. Dr. Jiang started his faculty career in Xiamen University after getting his Ph.D. degree and conducted postdoctoral researches with Prof. K. A. Zachariasse at Max-Planck-Institute for Biophysical Chemistry in Goettingen (Alexander von Humboldt research fellow) and Prof. Chi-Ming Che at the University of Hong Kong. Since 1995, he has been a full professor in the Department of Chemistry, Xiamen University and in 2004 was awarded the distinguished young investigator grant by NSF of China. He has been an invited professor in ENS Cachan of France and a visiting professor at National University of Singapore. He is on the editorial board of "Photochemical & Photobiological Science". His research has been focused on photophysics of electron/proton transfer and its applications for supramolecular fluorescent chemosensing and biointermolecular interactions.

References

1. Zietz, B. P.; de Vergara, J. D.; Dunkelberg, H., *Environ. Res*. **2003**, *92*, 129–138
2. Krämer, R., *Angew. Chem. Int. Ed*. **1998**, *37*, 772–773
3. Ghosh, P.; Bharadwaj, P. K.; Mandal, S.; Ghosh, S., *J. Am. Chem. Soc*. **1996**, *118*, 1553–1554
4. Dujols, V.; Ford, F.; Czarnik, A. W., *J. Am. Chem. Soc*. **1997**, *119*, 7386–7387
5. Klein, G.; Kaufmann, D.; Schürch, S.; Reymond, J. L., *Chem. Commun*. **2001**, 561–562
6. Kaur, S.; Kumar, S., *Chem. Commun.* **2002**, 2840–2841
7. Sun, X. Y.; Wen, Z. C.; Jiang, Y. B., *Chin. J. Chem*. **2003**, *21*, 1335–1338
8. Wu, Q. Y.; Anslyn, E. V., *J. Am. Chem. Soc*. **2004**, *126*, 14682–14683
9. Kaur, S.; Kumar, S., *Tetrahedron Lett*. **2004**, *45*, 5081–5085
10. Xu, Z. C.; Qian, X. H.; Cui, J. N., *Org. Lett*. **2005**, *7*, 3029–3032
11. Xu, Z. C.; Xiao, Y.; Qian, X. H.; Cui, J. N.; Cui, D. W., *Org. Lett*. **2005**, *7*, 889–892
12. Martínez, R.; Zapata, F.; Caballero, A.; Espinosa, A.; Tárraga, A.; Molina, P., *Org. Lett*. **2006**, *8*, 3235–3238
13. Singhal, N. K.; Ramanujam, B.; Mariappanadar, V.; Rao, C. P., *Org. Lett*. **2006**, *8*, 3525–3528
14. Kim, S. H.; Kim, J. S.; Park, S. M.; Chang, S. K., *Org. Lett*. **2006**, *8*, 371–374
15. Xiang, Y.; Tong, A. J.; Jin, P. Y.; Ju, Y., *Org. Lett*. **2006**, *8*, 2863–2866
16. Mei, Y. J.; Bentley, P. A.; Wang, W., *Tetrahedron Lett*. **2006**, *47*, 2447–2449
17. Wen, Z. C.; Yang, R.; He, H.; Jiang, Y. B., *Chem. Commun*. **2006**, 106–108
18. Chen, X. Q.; Ma, H. M., *Anal. Chim. Acta* **2006**, *575*, 217–222
19. Park, S. M.; Kim, M. H.; Choe, J. I.; No, K. T.; Chang, S. K., *J. Org. Chem*. **2007**, *72*, 3550–3553
20. Lee, M. H.; Kim, H. J.; Yoon, S.; Park, N.; Kim, J. S., *Org. Lett*. **2008**, *10*, 213–216
21. Mu, L.; Shi, W.; Chang, J. C.; Lee, S. T., *Nano Lett*. **2008**, *8*, 104–109
22. Mashraqui, S. H.; Khan, T.; Sundaram, S.; Ghadigaonkar, S., *Tetrahedron Lett*. **2008**, *49*, 3739–3743
23. Sheng, R.; Wang, P.; Gao, Y.; Wu, Y.; Liu, W.; Ma, J.; Li, H.; Wu, S., *Org. Lett*. **2008**, *10*, 5015–5018
24. Kovács, J.; Mokhir, A., *Inorg. Chem*. **2008**, *47*, 1880–1882
25. Li, A. F.; He, H.; Ruan, Y. B.; Wen, Z. C.; Zhao, J. S.; Jiang, Q. J.; Jiang, Y. B., *Org. Biomol. Chem*. **2009**, *7*, 193–200
26. Chen, X. Q.; Jia, J.; Ma, H. M.; Wang, S. J.; Wang, X. C., *Anal. Chim. Acta* **2009**, *632*, 9–14
27. Singh, A.; Yao, Q.; Tong, L.; Still, W. C.; Sames, D., *Tetrahedron Lett*. **2000**, *41*, 9601–9605
28. Tang, B.; Niu, J.; Yu, C.; Zhuo, L.; Ge, J., *Chem. Commun*.

2005, 4184–4186

29. Shang, L.; Dong, S. J., *J. Mater. Chem*. **2008**, *18*, 4636–4640
30. Xia, Y.; Zhu, C., *Analyst* **2008**, *133*, 928–932
31. Torrado, A.; Walkup, G. K.; Imperiali, B., *J. Am. Chem. Soc*. **1998**, *120*, 609–610
32. Zheng, Y.; Huo, Q.; Kele, P.; Andreopoulos, F. M.; Pham, S. M.; Leblanc, R. M., *Org. Lett*. **2001**, *3*, 3277–3280
33. Zheng, Y.; Gattás-Asfura, K. M.; Konka, V.; Leblanc, R. M., *Chem. Commun*.**2002**, 2350–2351
34. Zheng, Y.; Cao, X.; Orbulescu, J.; Konka, V.; Andreopoulos, F. M.; Pham, S. M.; Leblanc, R. M., *Anal. Chem*. **2003**, *75*, 1706–1712
35. White, B. R.; Holcombe, J. A., *Talanta* **2007**, *71*, 2015–2020
36. Kierat, R. M.; Krämer, R., *Bioorg. Med. Chem. Lett*. **2005**, *15*, 4824–4827
37. Clark, M. A.; Duffy, K.; Tibrewala, J.; Lippard, S. J., *Org. Lett*. **2003**, *5*, 2051–2054
38. Gunnlaugsson, T.; Leonard, J. P.; Murray, N. S., *Org. Lett*. **2004**, *6*, 1557–1560
39. Kubo, Y.; Ishida, T.; Kobayashi, A.; James, T. D., *J. Mater. Chem*. **2005**, *15*, 2889–2895
40. Royzen, M.; Dai, Z.; Canary, J. W., *J. Am. Chem. Soc*. **2005**, *127*, 1612–1613
41. Varazo, K.; Xie, F.; Gulledge, D.; Wang, Q., *Tetrahedron Lett*. **2008**, *49*, 5293–5296
42. Liao, Q. X.; Li, A. F.; Li, Z.; Jiang, Y. B., *Chem. J. Chinese Univ*. **2008**, *29*, 2531
43. Demas, J. N.; Crosby, G. A., *J. Phys. Chem*. **1971**, *75*, 991–1024
44. Gunnlaugsson, T.; Lee, T. C.; Parkesh, R., *Org. Biomol. Chem*. **2003**, *1*, 3265–3267
45. Ono, A.; Togashi, H., *Angew. Chem. Int. Ed*. **2004**, *43*, 4300–4302
46. Liu, J.; Lu, Y., *Angew. Chem. Int. Ed*. **2007**, *46*, 7587–7590
47. Grabowski, Z. R.; Rotkiewicz, K.; Rettig, W., *Chem. Rev*. **2003**, *103*, 3899–4032